

Partonic collectivity in high-energy nuclear collisions

Nu Xu

Nuclear Science Division

Lawrence Berkeley National Laboratory, 1 Cyclotron Road, CA 94720, USA

E-mail: NXu@lbl.gov

Abstract. After a brief introduction to the physics of high-energy nuclear collisions, we will present recent experimental results that are closely connected to the properties of the matter produced in Au+Au collisions at RHIC. Collective motion with parton degrees of freedom is called partonic collectivity. We will focus on collective observables such as transverse radial flow and elliptic flow. With experimental observations, we will demonstrate that, at RHIC, collectivity has already been developed prior to the hadronic stage. Finally, we will develop a plan for future measurements that are needed for characterization of the partonic Equation of State in high-energy nuclear collisions.

1. Introduction

This is my first trip to India. I am very grateful to the conference organizers. India, as I was taught when I was young, is a great land with a long history of civilization. One of the few quotations I recite often is this: *“Each soul is potentially divine. The goal is to manifest this divinity within by controlling nature: external and internal. Do this either by work, or worship, or psychic control, or philosophy - by one, or more, or all of these - and be free.”* – S. Vivekananda. I do believe in *work*. I believe this short trip is the beginning of a long journey toward happiness.

The purpose of the high-energy nuclear collision program at both Brookhaven National Laboratory (BNL) and CERN is to probe strongly interacting matter under extreme conditions, *i.e.* at high densities and temperatures. Naturally the search for the existence of a new form of matter - the matter with partonic equation of state (EOS) that colloquially called quark-gluon plasma - is the experimental focus of the program. It has been demonstrated that the flow measurement is one of the most powerful methods for studying partonic EOS in high-energy nuclear collisions. For recent reviews, see [1, 2] and references therein.

The term flow has two important aspects: (i) collectivity of produced hadrons and (ii) the local thermalization among these hadrons [3]. As long as there are interactions among constituents, collectivity of the matter will be developed provided that the distribution of matter density is inhomogeneous. When the interactions last long enough the system will eventually approach local equilibrium and hence develops hydrodynamic type flow. At the early stage of a high-energy nuclear collision, both the matter density and its gradient are large, therefore we expect the development of partonic collectivity - the collective motion of partons. The issues of partonic local equilibrium can be addressed by studying heavy-flavor (*c*-, *b*-quarks) collectivity.

This is because the collisions that generate the collective motion for heavy-quarks will likely lead to thermalization among the light quarks (u -, d -, s -quarks). It is important to note that collectivity is cumulative through the expansion phase and is not affected by the details of the hadronization process.

This paper is organized as follows: First we will discuss the results of hadron transverse momentum spectra. The freeze-out thermodynamic parameters (T_{fo} , β_T) as a function of collision centrality will be discussed. Comparing with the results of π , K , and p , we will show that multi-strange hadrons like the ϕ and Ω freeze-out at a relatively earlier time with a higher temperature and smaller collective velocity. In section 3, we will discuss the event anisotropy parameter v_2 . Since the multi-strange hadrons Ξ and Ω have demonstrated the $v_2(p_T)$ is similar to other baryon's $v_2(p_T)$, we will argue that the collectivity has been developed before hadronization. The first result of the open-charm v_2 , as observed in the electron decayed channel, will be presented in section 4 and a brief summary will be given in section 5.

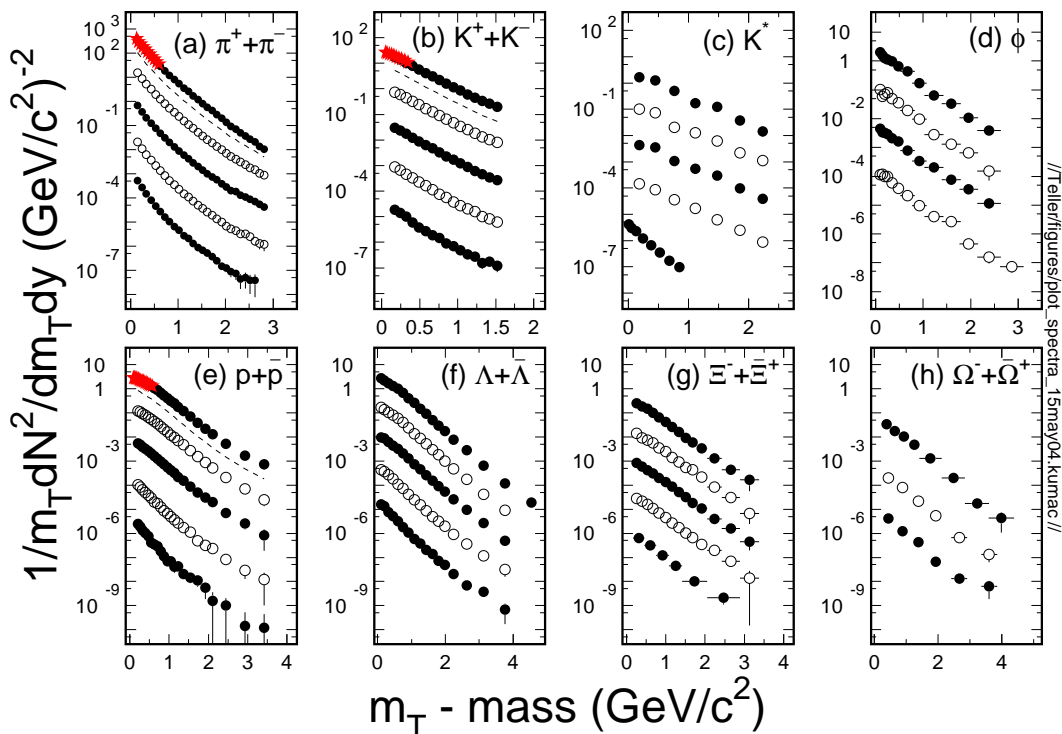


Figure 1. Mid-rapidity hadron spectra from $\sqrt{s_{NN}} = 200$ GeV $Au + Au$ and $p + p$ collisions. Most and least central collisions are listed from top-down. For pions (a), kaons (b), and protons (e) [4], the centrality bins are: 0-5%, 20-30% (10^{-1}), 40-50% (10^{-2}), 60-70% (10^{-3}), and 80-92% (10^{-4}). The star symbols (0-5%) are data from [5]. The dashed-lines represent the spectra from minimum biased collisions. For K^* (c) [6], from top to bottom, respectively, the centralities are 0-10%, 10-30%, 30-50%, 50-80% for $Au + Au$ collisions and $p + p$ collisions. For ϕ -meson (d) [7], the centralities are: 0-5%, 10-30% (10^{-1}), 30-50% (10^{-2}), and 50-80% (10^{-3}). For Λ (f) and Ξ (g) [8], the centrality bins are: 0-5%, 10-20% (10^{-1}), 20-40% (10^{-2}), 40-60% (10^{-3}), 60-80% (10^{-4}). For the Ω baryon (h) [8], the centralities are: 0-10%, 20-40% (2×10^{-2}), and 40-60% (10^{-3}).

2. Transverse momentum distributions - collective expansion

In Figure 1, the mid-rapidity transverse momentum distributions (the invariant spectra are plotted as a function of $m_T - \text{mass}$) for pions, kaons, protons [4], K^* [6], ϕ [7], Λ , Ξ , and Ω

[5, 8], from $\sqrt{s_{NN}} = 200$ GeV $Au + Au$ and $p + p$ collisions, are shown. While pion spectra show a p_T -power-law shape, most of the hadron spectra are m_T -exponential, especially the strange hadrons like K , ϕ , Ξ and Ω . In order to characterize the transverse motion, an exponential fit or a power-law fit is often used for the measured spectra. In addition, for spectra extracted from heavy ion collisions, hydrodynamics motivated fits [9] are applied.

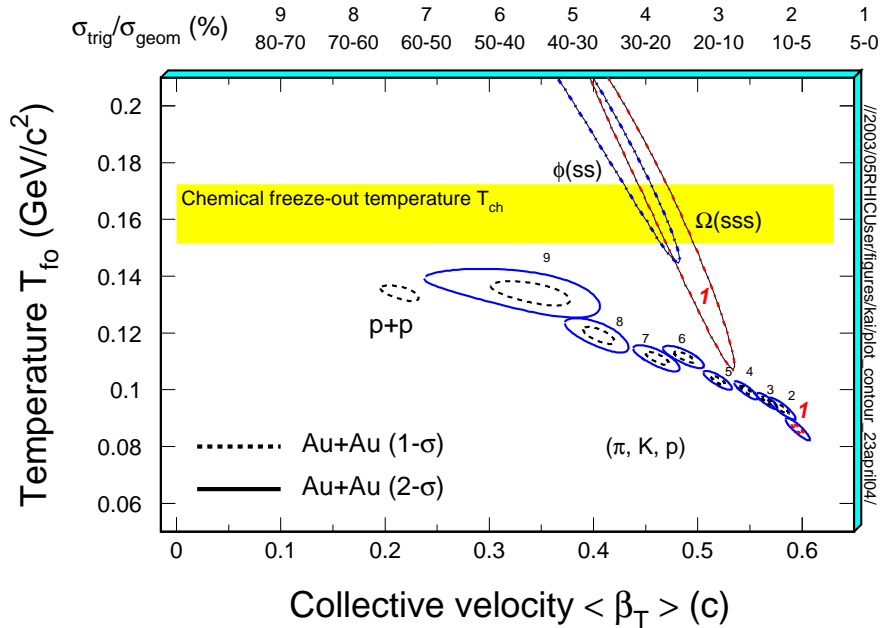


Figure 2. χ^2 contours, extracted from the thermal+radial flow fits, for copiously produced hadrons π, K and protons and multi-strange hadrons ϕ and Ω . On the top of the plot, the numerical labels indicate the centrality selection. For π, K and protons, 9 centrality bins (from top 5% to 70-80%) were used from 200 GeV $Au+Au$ collisions. The results from 200 GeV $p + p$ collisions are also shown. For ϕ and Ω , only the most central results are presented. Dashed- and solid-lines are the 1- σ and 2- σ contours, respectively.

The thermal fits allow us to construct common freeze-out contours, for a given group of hadrons, in the $(T_{fo}, \langle \beta_T \rangle)$ plane. In this approach, the thermal random motion and ordered collective motion are separated [9, 10]. The χ^2 contours are extracted from the thermal + radial flow fits and presented in the temperature-velocity space. Figure 2 shows a qualitatively different behavior, in the temperature versus collective velocity plane, between the relatively rarely produced multi-strange particles and copiously produced particles π, K and p . On top of the plot, the numerical labels indicate the centrality selection. For π, K and protons, 9 centrality bins were used from the 200 GeV $Au + Au$ collisions and $p + p$ collisions [5]. For ϕ and Ω , only the most central results are shown. Dashed- and solid-lines are the 1- σ and 2- σ contours, respectively.

As the centrality increases from peripheral to central collisions, for copiously produced hadrons, π, K, p , the values of the temperature parameter decreases and the velocity parameter increases. At the most central collisions, the velocity becomes as high as 60% of the speed of light and the thermal freeze-out temperature is at ~ 100 MeV. On the other hand, the fit results indicate that the minima for multi-strange hadrons are not sensitive to collision centrality and they are all close to a temperature of $T \sim 160 - 170$ MeV and an average velocity of $\langle \beta_T \rangle \sim 0.4c$. Note that this temperature is the same as the chemical freeze-out temperature [11, 12, 13, 14] and it is close to the value of the phase transition temperature [15]. Due to relatively small total hadronic cross sections [16, 17, 18, 19] and their heavy mass, multi-strange particles do

not participate in the evolution of the system during the hadronic phase. As a result, they de-associate from the system near the hadronization point with $T_{fo} \sim 170$ MeV and $\beta_T \sim 0.4c$. The finite value of the collective velocity must have been developed before the hadronization - the partonic collectivity.

Two short notes regarding to the contour plot Fig. 2 are in order:

(1) The direct measurements of the cross section from the multi-strange hadron and nucleon interactions are scarce. Early study of photo-production of ϕ -meson has concluded a relatively small cross section of $\phi + p$ interaction, although the result is model dependent [20]. Recent report from the $\Xi^- + p$ elastic and inelastic scatterings concluded a relatively a small value of cross section [21]. In addition, I would argue that the Fig. 2 is a measure of the effective interaction cross sections in heavy ion collisions. Since there is either no or small number of high state of resonances for most of the multi-strange hadrons and the mass of the ϕ -meson is very close to that of the protons, the observation of the different freeze-out time between ϕ -meson and protons, for example, has to come from the difference in the strength of the interaction. The claim [22] of a common hydrodynamic model fit to all particle species from Au+Au collisions at RHIC, including the Ω baryons, is not supported by the experimental observations. Besides other problems, the treatment of freeze-out in the hydrodynamic model alone is not adequate.

(2) As one can see in the figure that there is finite velocity in $p + p$ collisions at $\sqrt{s_{NN}} = 200$ GeV. Thermal model fit tests show that it is caused by the jet production [23] in the high energy collisions. In principle, such jetiness-collectivity, caused by large momentum transfer, is different from the hydrodynamic type of collectivity discussed above. In central $Au + Au$ collisions, the collective effect arise from the jet production is probably small due to the severe energy loss in the medium [24].

3. Elliptic flow v_2 – Evidence for partonic collectivity at RHIC

The particle azimuthal distribution with respect to the reaction plane at a given rapidity window can be de-convoluted by the expansion:

$$\frac{dN}{d\phi} \approx v_0(1 + 2v_1 \cos(\Delta\phi) + 2v_2 \cos(2\Delta\phi)). \quad (1)$$

The first and second Fourier coefficients, v_1 and v_2 , are connected to direct flow and elliptic flow, respectively. The coefficient v_0 is a normalization constant and $\Delta\phi$ is defined as the azimuthal angle difference between the particle and the event reaction plane. At a given rapidity the coefficients are: $v_1 = \langle \cos(\Delta\phi) \rangle$ and $v_2 = \langle \cos(2\Delta\phi) \rangle$. Because the rescattering induced expansion naturally reduces the spatial anisotropy, the early information of the collision dynamics can be learned through measuring v_1 , v_2 and higher order harmonics [25, 26, 27, 28].

The measured elliptic flow v_2 from the minimum bias $Au + Au$ collisions at $\sqrt{s_{NN}} = 200$ GeV for π, K_0^S, p, Λ [29, 30] are shown in Figure 3 (a). Respectively, from top to bottom the dashed-lines represent the elliptic flow of $\pi, K, p, \Lambda, \Xi, \Omega$ from hydrodynamic calculations [31]. In the low p_T region, the trends of v_2 are well reproduced by the hydrodynamic calculations. At higher p_T , the v_2 is found to be saturated and hydrodynamic results over-predict the data. While the baryons saturate at $p_T \geq 3$ GeV/c with $v_2 \sim 0.2$, mesons saturation starts earlier at lower values of v_2 .

Figure 3 (b) and (c) show v_2 for the multi-strange baryons $\Xi^- + \Xi^+$ and $\Omega^- + \Omega^+$ [8, 32], respectively. Although they tend to suffer much less rescatterings during the later hadronic stage of the collisions [16], the values of v_2 for strange-baryons, within the experimental uncertainties, are found to be as high as other hadrons at a given p_T . Therefore, the v_2 must have been developed at an earlier stage prior to hadronization. This measurement and the early freeze-out

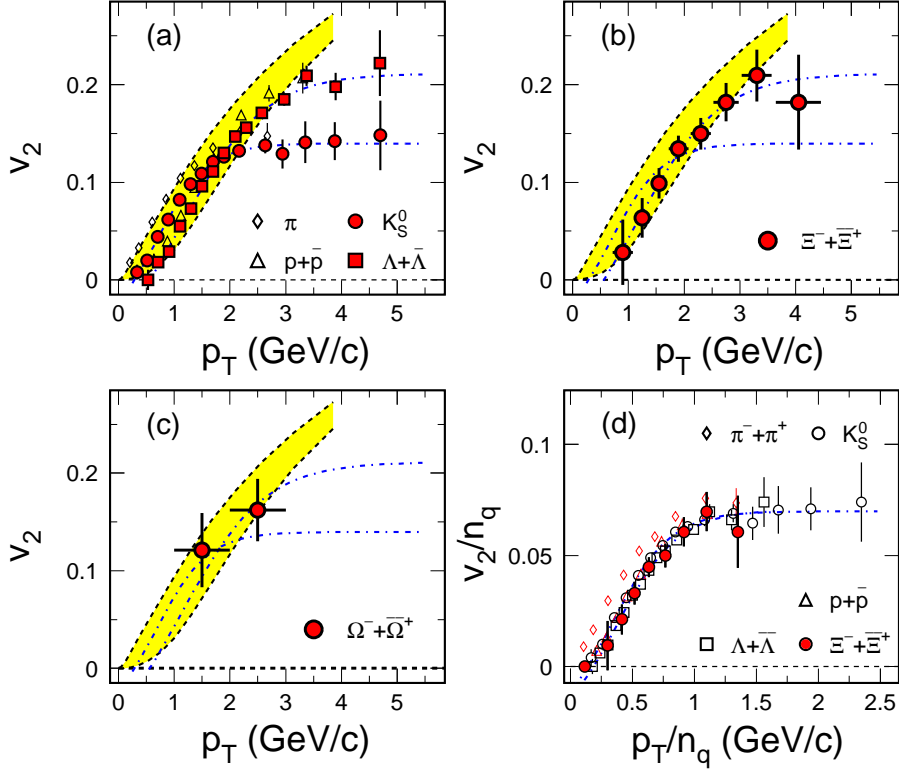


Figure 3. (a) Experimental results of the transverse momentum dependence of the event anisotropy parameters for π , K_S^0 , $p + \bar{p}$, $\Lambda + \bar{\Lambda}$ [30, 29]. Hydrodynamic calculations are shown as thick-dashed-lines. From top to bottom are the results for π , K , p , Λ , $\Xi^- + \Xi^+$, and $\Omega^- + \Omega^+$; Multi-strange baryon elliptic flow v_2 are shown in (b) for Ξ and (c) for Ω . Plots (b) and (c) are from preliminary STAR results [8, 32]. (d) Number of constituent quark (n_q) scaled v_2/n_q versus scaled p_T/n_q . All curves are from [33].

(see Fig. 2) for the multi-strange hadrons constitute a clear piece of evidence for the development of partonic collectivity in $Au + Au$ collisions at RHIC.

The measured v_2 distributions have been fitted with the equation given as [33]:

$$f_{v_2} = \frac{a}{1 + \exp(-(x - b)/c)} - d, \quad (2)$$

where parameters a , b , c and d are fixed from the fit. The fit results to K_S^0 and Λ are shown as dot-dashed lines in Fig. 3. According to coalescence approaches [34], after scaling both values of v_2 and p_T with the number of the constituent quarks (NCQ) of the corresponding hadron, all particles should fall onto one single curve. Fig. 3(d) shows the scaled v_2 versus the scaled p_T . Indeed, with the exception of pions, all particles follow a single curve. This observation implies that due to high parton density and intense interactions partons have already developed collective motion in heavy ion collisions at RHIC.

In the NCQ scaled plot, Fig. 3(d), the fit results are shown as dashed lines. For kaon, proton and lambda, the scaling seems to be working within $p_T/n_q \leq 2.5$ GeV/c. Pions (open triangles) do not follow the scaling, because of a large fraction of hadrons produced through resonance decays. This is particularly true for pions in high-energy heavy ion collisions [35, 36]. At mid-rapidity, in collisions at RHIC, as high as $\sim 80\%$ of pions are from resonance decays and the dominant sources for pion production are ρ , ω and baryon resonances like Λ and Δ .

4. Heavy-flavor collectivity - light-flavor thermalization at RHIC

In the previous sections, we established the evidence of partonic collectivity for light-flavor (u , d , s) hadrons. In order to access the partonic EOS, one must address the issue of early excitation/thermalization [37] of the system. Because the masses of heavy-flavors are much larger than the highest possible excitation of the system reached in $Au + Au$ collisions at RHIC, a large number of rescatterings would be required in order to develop any collective motion. Furthermore, since the number density of light-flavors is much higher than that of heavy-flavors, the intensity of rescattering should be even stronger among the light-flavors. As expected for any physical system, intensive rescattering among constituents will eventually lead to thermalization. Therefore, the heavy-flavor collectivity could be used to probe the intensity of partonic rescattering and therefore the degree of light-flavor thermalization. In practice, this means that we should measure the v_2 of charm-hadrons [33, 38, 39, 40, 41].

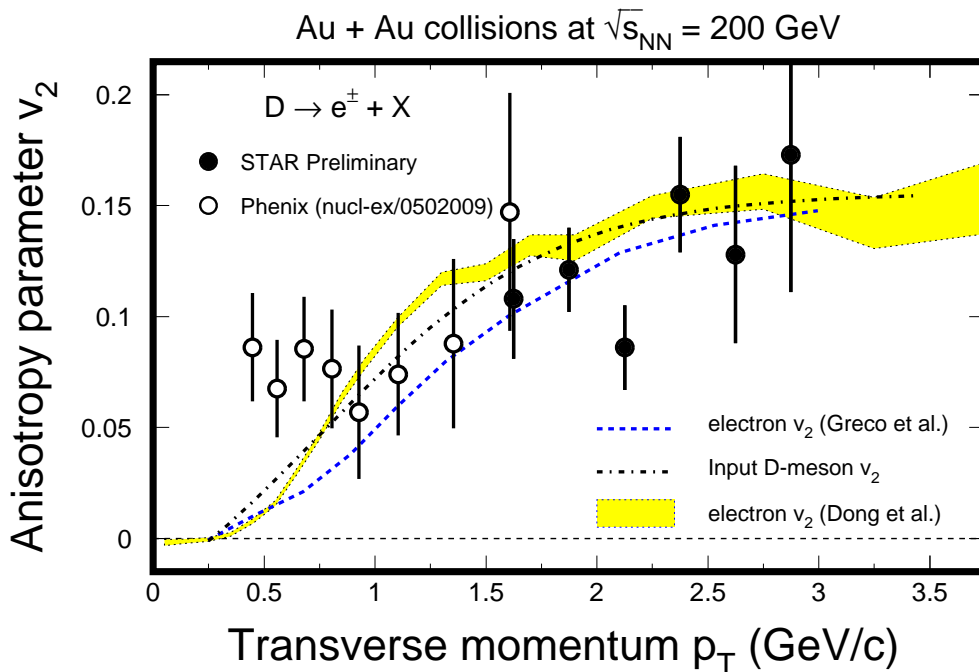


Figure 4. Non-photonic electron elliptic flow $v_2(p_T)$ from minimum bias $Au + Au$ collisions at $\sqrt{s_{NN}} = 200$ GeV. Data from PHENIX [43] and STAR [45] experiments are shown as open- and filled-circles, respectively. Only statistical errors are shown. Dashed-line and the hatched band are charm-hadron decayed electron $v_2(p_T)$ from refs. [33, 38].

The heavy-flavor program has just started at RHIC [42] and there is no measurement of v_2 with reconstructed charm-hadron yet. However, as discussed in [33, 38], the charm-hadron v_2 can be inferred by their decayed electron v_2 . The results of the non-photonic electron v_2 from minimum bias $Au + Au$ collisions at $\sqrt{s_{NN}} = 200$ GeV [43, 44, 45] are shown in Figure 4. These non-photonic electrons are presumably from the decays of charm-hadrons. Only statistical errors are shown in the figure and the systematic errors are in the order of 25%. The dashed-line and hatched-band are charm-hadron decayed electrons from model calculations [38, 33]. The dot-dashed-line [33] is the D-meson v_2 assuming NCQ-scaling. Since there are several resonance states for charm-hadrons, hadronic interactions could also develop non-vanishing v_2 [39, 40]. A recent study based on the HSD model indeed shows the value of maximum v_2 in the order of 2-3% [39] in the $b=7$ fm $Au + Au$ collisions at RHIC. Due to the large statistical uncertainties in data, both model results are consistent with the measurements. The observation indicates, if confirmed

with (high statistics) reconstructed charm-hadron measurements, the onset of collectivity for the heavy-flavors and the light-flavor thermalization at RHIC.

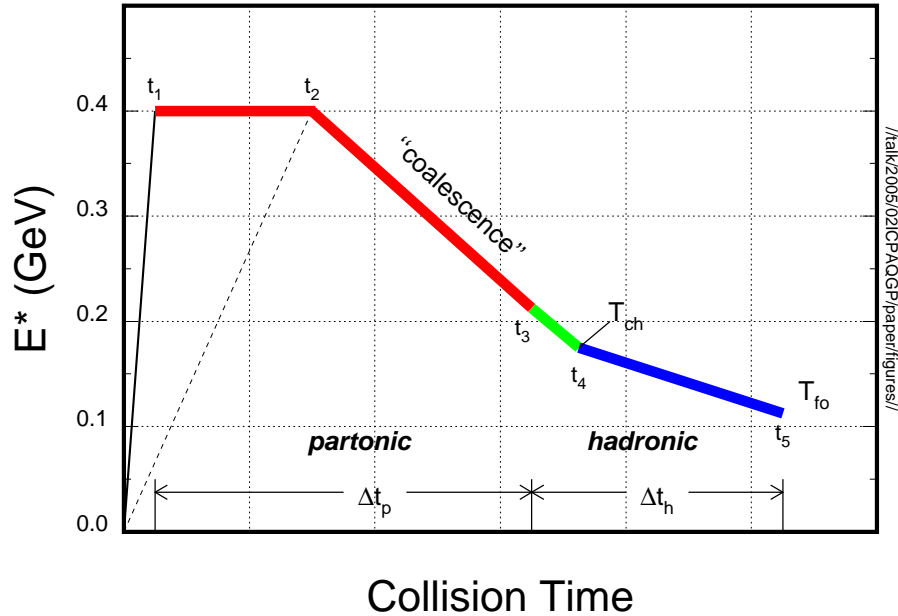


Figure 5. Excitation of high-energy nuclear collision as a function of time. In case of thermalization, E^* has the meaning of a temperature T .

Assuming the system has reached thermalization at the early stage, now the questions are: What is the temperature? How long does the system stay at the equilibrium? More importantly: How does the transformation from a partonic system to a hadronic system occur? What are the dynamics for hadron mass formation?

Figure 5 is a schematic time evolution of the system in high-energy nuclear collisions. The important realization here is that, in both partonic and hadronic periods, collective expansion occurred. During the partonic period (Δt_p) interactions are dominated by quarks and gluons. During t_2 and t_3 , the temperature T is in the order of T_c and colored bound states [46, 47] are coalesced. Since gluons are disappearing and giving their way to massive quarks, the degrees of freedom are gradually reduced. At the same time, both quarks and the colored bound-states are acquiring mass. In order to avoid the shrinking of entropy, the system is expanding rapidly – further enhancing the partonic collectivity. Near the end of the period, colorless hadrons are formed. The duration between t_3 and t_4 is expected to be small and most of hadrons are born in a state of chemical equilibrium. Later, the hadronic interactions during Δt_h lead to further expansion and cooling of the system until the kinetic freeze-out. Hadronic observables have allowed us to extract information as early as $t \leq t_3$. However, earlier dynamic information of the system, which answers the first two questions, one has to extract from photon and low mass di-lepton measurements. RHIC detector upgrades are necessary in order to perform these measurements with high precision.

Acknowledgments: I am thankful for many enlightening discussions with Drs. P. Braun-Munzinger, J.E. Gonzalez, M. Gyulassy, U. Heinz, P. Huovinen, F. Liu, M. Oldenburg, A. Poskanzer, H.G. Ritter, K. Schweda, P. Sorensen, E.V. Shuryak, Z. Xu, and P.F. Zhuang. This work has been supported by the U.S. Department of Energy under Contract No. DE-AC03-

- [1] H.G. Ritter and X.N. Wang, proceedings of “*Quark Matter 2004*”, J. Phys. **G30**, (2004) and references therein.
- [2] RHIC experiments whitepapers: nucl-ex/0410020 (BRAHAMS); nucl-ex/0410003 (PHENIX); nucl-ex/0410022 (PHOBOS); nucl-ex/0501009 (STAR).
- [3] W. Reisdorf and H.G. Ritter, Ann. Rev. Nucl. Part. Sci. **47**, 663(1997).
- [4] S.S. Adler *et al.*, (PHENIX Collaboration), Phys. Rev. **C69**, 034909(2004).
- [5] J. Adams *et al.*, (STAR Collaboration), Phys. Rev. Lett. **92**, 112301(2004).
- [6] J. Adams *et al.*, (STAR Collaboration), subm. to Phys. Rev. **C**, December, 2004. nucl-ex/0412019.
- [7] J. Adams *et al.*, (STAR Collaboration), nucl-ex/0406003 and E. Yamamoto, (STAR Collaboration), Nucl. Phys. **A715**, 466c(2003).
- [8] K. Schweda *et al.*, (STAR Collaboration), J. Phys. G: Nucl. Part. Phys. **30**, S693(2004).
- [9] E. Schnedermann, J. Sollfrank, and U. Heinz, Phys. Rev. **C48**, 2462(1993).
- [10] I. G. Bearden *et al.*, (NA44 Collaboration), Phys. Rev. Lett **78**, 2080(1997).
- [11] P. Braun-Munzinger, J. Stachel, J. Wessels, and N. Xu, Phys. Lett. **B344**, 43(1995); P. Braun-Munzinger, I. Heppe, and J. Stachel, Phys. Lett. **B465**, 15(1999).
- [12] P. Braun-Munzinger, these proceedings.
- [13] J. Cleymans and K. Redlich, Phys. Rev. Lett. **81**, 5284(1998).
- [14] N. Xu and M. Kaneta, Nucl. Phys. **A698**, 306c(2001).
- [15] F. Karsch, Nucl. Phys. **A698**, 199c(2002).
- [16] H. van Hecke, H. Sorge, and N. Xu, Phys. Rev. Lett. **81**, 5764(1998).
- [17] Y. Cheng, F. Liu, Z. Liu, K. Schweda, and N. Xu, Phys. Rev. **C68**, 034901(2003).
- [18] C. Alt *et al.*, (NA49 Collaboration), sub. Phys.Rev.Lett., Sept. 2004; nucl-ex/0409004
- [19] M. Bleicher, these proceedings.
- [20] H.-J Behrend *et al.*, Phys. Lett. **B56**, 408(1975).
- [21] J.K. Ahn *et al.*, sub. to Phys. Lett. **B**, nucl-ex/0502010.
- [22] U. Heinz, these proceedings.
- [23] Zhixu Liu, in preparation, February 2005.
- [24] C. Adler *et al.*, (STAR Collaboration) Phys. Rev. Lett. **90**, 082302(2003).
- [25] H. Sorge, Phys. Lett. **B402**, 251(1997).
- [26] J.-Y. Ollitrault, Phys. Rev. **D46**, 229(1992).
- [27] S. Voloshin, Nucl. Phys. **A715**, 379c(2003).
- [28] J. Adams *et al.*, (STAR Collaboration) Phys. Rev. Lett. **92**, 062301(2004).
- [29] J. Adams, *et al.*, (STAR Collaboration), Phys. Rev. Lett. **92**, 052302(2004).
- [30] S.S. Adler *et al.*, (PHENIX Collaboration), Phys. Rev. Lett. **91**, 182301(2003).
- [31] P. Huovinen, P. Kolb, U. Heinz, P.V. Ruuskanen, and S. Voloshin, Phys. Lett. **B503**, 58(2001).
- [32] J. Castillo *et al.*, (STAR Collaboration), J. Phys. G: Nucl. Part. Phys. **30**, S1207(2004).
- [33] X. Dong, S. Esumi, P. Sorensen, N. Xu, and Z. Xu, Phys. Lett. **B597**, 328(2004).
- [34] Z. Lin and C. Ko, Phys. Rev. Lett. **89**, 202302(2002); R.J. Fries, B. Mueller, C. Nonaka, S.A. Bass, Phys. Rev. Lett. **90**, 202303(2003); D. Molnar and S. Voloshin, Phys. Rev. Lett. **91**, 092301(2003).
- [35] Zhang-bu Xu, nucl-ex/0307014, (2003).
- [36] R.J. Fries, B. Mueller, C. Nonaka, S.A. Bass, Phys. Rev. **C68** 044902(2003); C. Nonaka, B. Mueller, M. Asakawa, S.A. Bass, and R.J. Fries, Phys. Rev. **C69**, 031902(2004).
- [37] H. Stöcker, Nucl. Phys. **A750**, 121(2005) and these proceedings.
- [38] V. Greco, C. M. Ko, R. Rapp, Phys. Lett. **B595**, 202(2004).
- [39] E.L. Bratkovskaya, W. Cassing, H. Stöcker, N. Xu, Phys.Rev. **C**, in print; nucl-th/0409047.
- [40] H. van Hees and R. Rapp, Phys. Rev. **C71**, 034907(2005).
- [41] X.L. Zhu, P.F. Zhuang and N. Xu, Phys. Lett. **B607**, 107(2005).
- [42] J. Adams, *et al.*, (STAR Collaboration), Phys. Rev. Lett. **94**, 062301(2004).
- [43] M. Kaneta *et al.* (PHENIX Collaboration), J. Phys. **G30**, S1217(2004); S.S. Adler *et al.* (PHENIX Collaboration), nucl-ex/0502009.
- [44] H. Hamagaki, these proceedings.
- [45] F. Laue *et al.* (STAR Collaboration), nucl-ex/0411007.
- [46] E. Shuryak and I. Zahed, Phys. Rev. **C70**, 021901(2004); Phys. Rev. **D69**, 046005(2004); these proceedings.
- [47] Hong-Jo Park, Chang-Hwan Lee, and Gerald E. Brown, hep-ph/0503016.